Journal of Luminescence 131 (2011) 1368–1375

Contents lists available at ScienceDirect

Journal of Luminescence

journal homepage: www.elsevier.com/locate/jlumin

Absorption and fluorescence studies of Sm^{3+} ions in lead containing sodium fluoroborate glasses

C. Madhukar Reddy [a], G.R. Dillip [a], K. Mallikarjuna [a], Sd. Zulifiqar Ali Ahamed [a], B. Sudhakar Reddy [b], B. Deva Prasad Raju [c,*]

[a] Department of Physics, Sri Venkateswara University, Tirupati 517502, India
[b] Department of Physics, Sri Venkateswara Degree College, Kadapa 516003, India
[c] Department of Future Studies, Sri Venkateswara University, Tirupati 517 502, India

ARTICLE INFO

Article history:
Received 22 December 2010
Accepted 8 March 2011
Available online 15 March 2011

Keywords:
Glasses
Rare earths
Judd–Ofelt theory
Fluorescence
Lifetimes
Energy transfer

ABSTRACT

Lead containing calcium zinc sodium fluoroborate glasses (LCZSFB) with molar composition of $20PbO+5CaO+5ZnO+10NaF+(60-x)\ B_2O_3+x\ Sm_2O_3$, ($x$=0.1, 0.25, 0.5, 1.0 and 2.0 mol%) were prepared and investigated by the XRD, FTIR, optical absorption, photoluminescence and decay curve analysis. Judd–Ofelt theory was applied to the experimental oscillator strengths to evaluate the phenomenological *J–O* intensity parameters Ω_λ (λ=2, 4 and 6). Using the *J–O* intensity parameters as well as from the emission and decay measurements, various radiative parameters such as transition probabilities (A_R), radiative lifetimes (τ_R), measured lifetimes (τ_m), calculated branching ratios (β_R), measured branching ratios (β_m), effective bandwidth ($\Delta\lambda_{eff}$) and stimulated emission cross sections $\sigma(\lambda_p)$ have been calculated for the excited $^4G_{5/2}$ luminescent level. The nature of decay curves of $^4G_{5/2}$ level for different Sm^{3+} ion concentrations in all LCZSFB glasses has been analyzed and the lifetimes are noticed to decrease with increase of concentration. The concentration quenching has been attributed to the energy transfer through the cross-relaxation between Sm^{3+} ions. Based on these results, the utility of Sm^{3+} ions doped lead containing fluoroborate glasses as laser active materials in the visible region is discussed.

1. Introduction

Over the past several years, trivalent lanthanide ions doped heavy metal oxide based glasses have been prepared and investigations on the optical absorption and fluorescence studies of these glasses are found wide commercial applications in the fields of lasers and telecommunications. Efficient laser hosts can be realized using heavy metal oxide glasses in view of their low phonon energy [1]. Host glasses with low phonon energies allow large radiative transition rates that are useful for the design and development of optical devices such as up converters, light emitting diodes (LEDs), fiber amplifiers, memory devices, etc. In this direction, a great amount of research has been carried out to develop new glass matrices containing rare earth (RE) ions.

Borate glasses show clear relationship between glass structure and physical properties, high transparency, low melting point, high thermal stability and good glass forming nature have been identified as more useful host matrices to accommodate the required quantity of rare earth ions compared to several other conventional glassy systems [2–4]. Borate glasses incorporated by heavy metal oxides can give intense fluorescence in the visible spectral region which is used as electro-optic modulators, electro-optic switches, solid-state laser materials and non-linear parametric converters [5–8]. In recent years, a special interest has been evinced towards the production of fluoroborate glasses due to their high ionic conductivity, the short range order around the network forming borons, anomalous dependence of their structure on the molar fraction of oxide modifiers, the special role of the fluoride ions in the formation of the three dimensional network and their potential use in the production of infrared optical components. In addition, fluoride compounds possess attractive features in the field of quantum electronics by virtue of their excellent physical and chemical properties, high stability with respect to short wavelength radiation, low phonon cut-off frequencies and transparency in the wide spectral region. Presence of fluorides shifts the IR cut-off edge towards larger wavelengths making them suitable for fiber amplifiers [9,10], which are used in telecommunications and strongly reduces OH absorption [11] because fluorine might react with the OH group to form HF. Thus, these heavy metal oxide fluoroborate glass systems could work as good fluorescent host matrices and the boron oxygen groups dominantly contribute for their potential uses in the optoelectronic and nonlinear applications.

* Corresponding author: Tel.: +91 94402 81769.
E-mail address: drdevaprasadraju@gmail.com (B. Deva Prasad Raju).

0022-2313/$ - see front matter © 2011 Elsevier B.V. All rights reserved.
doi:10.1016/j.jlumin.2011.03.016

Among RE ions, the Sm^{3+} ion is one of the most interesting ions for analyzing the fluorescence properties because of its use in high density optical storage, under sea communication, color displays and visible solid-state lasers. Sm^{3+} ion with $4f^5$ electronic configuration exhibit a strong orange–red fluorescence in the visible region. Mahto et al. [12] reported the concentration quenching of fluorescence of $^4G_{5/2}$ level and attributed it to quadrupole–quadrupole interaction among the Sm^{3+} ions. The concentration quenching of the $^4G_{5/2}$ fluorescence has been analyzed in different glasses which include fluoroborate [12], fluorozirconate [13], germanate [14] and tellurite [15] glasses at ambient conditions. Especially, glasses doped with Sm^{3+} ions were extensively investigated by optical spectroscopy to characterize these materials for optical devices applications [16,17].

From earlier studies, it is known that the fluorescence is highly concentration dependent and is often quenched. Thus, for optimum results host dependent as well as concentration dependent studies of the fluorescence of Sm^{3+} are essential. In the present work, we have studied the absorption, fluorescence and decay processes of Sm^{3+} ions with different concentrations in LCZSFB glasses. From the absorption analysis, the radiative lifetimes and branching ratios for different excited levels have been obtained by applying the Judd–Ofelt theory [18,19] and are compared with the experimental results. The decay characteristic of $^4G_{5/2}$ level of Sm^{3+} ion has also been recorded and analyzed. The phenomenon of concentration quenching and the involved mechanism have been discussed. An attempt was made to assess the potential of Sm^{3+} doped LCZSFB glasses as laser active materials.

2. Experimental method

The chemical composition of different concentrations of Sm^{3+}-doped LCZSFB: $20PbO+5CaO+5ZnO+10NaF+(60-x)\ B_2O_3+x\ Sm_2O_3$, where $x=0.1$, 0.25, 0.5, 1.0 and 2.0 mol% glasses were prepared by the melt quenching method. Approximately 10 g batches of chemicals were mixed and grinded in required proportions in an agate mortar. The mixture was taken into a porcelain crucible and kept for melting at a temperature of 950 °C in high temperature furnace at ambient atmosphere. After 1 h, the melt was quenched on a pre-heated brass plate at 360 °C and are kept for annealing for 8 h at the same temperature to remove the thermal strains occurred during the sudden quench to get good mechanical stability. The glasses were shaped and polished to measure their physical and optical properties.

For 1.0 mol% Sm^{3+}-doped LCZSFB glass sample, the density (4.98 g/cc) was determined by the Archimedes method, using distilled water as the immersion liquid. The thickness (optical path length) (0.28 cm) was measured by a screw gage and the refractive index of 1.590 was measured using Abbe's refractometer at sodium wavelength with 1-bromonapthalene ($C_{10}H_7Br$) as the contact liquid. The concentration of Sm^{3+} ions in 1.0 mol% Sm^{3+} doped LCZSFB glass is found to be 1.575×10^{20} ions/cc. The various physical properties of the 1.0 mol% Sm^{3+}-doped glasses are presented in Table 1. The X-ray diffraction (XRD) profile using Seifert X-ray diffractometer and FTIR spectrum in the range 450–4000 cm^{-1} using Perkin–Elmer Spectrum One FTIR spectrophotometer was recorded.

Room temperature, visible and near infrared absorption spectra for 1.0 mol% Sm^{3+}-doped LCZSFB glass were recorded using Varian Cary 5E UV–vis–NIR spectrophotometer in the 450–1800 nm wavelength region. The excitation and fluorescence spectra were recorded using Jobin Vyon Fluorolog-3 spectrofluorometer with xenon flash lamp as source. Lifetimes of the $^4G_{5/2}$ excited level for different concentrations of Sm^{3+} ions were also measured with 402 nm excitation wavelength by using Jobin Vyon Fluorolog-3 spectrofluorometer.

Table 1
Measured physical properties for 1.0 mol% Sm^{3+}-doped LCZSFB glass.

Physical quantities	LCZSFB
Sample thickness (cm)	0.280
Refractive index (n)	1.590
Density (g/cc)	4.980
Concentration (mol/mol)	0.262
Concentration (ions $cm^{-3}\times10^{20}$)	1.575
Average molecular weight (g)	190.400
Dielectric constant (ε)	2.530
Molar volume V_m (cm^3/mol)	38.220
Glass molar refractivity (cm^{-3})	12.910
Electronic polarizability α_e ($\times10^{-24}$ cm^3)	5.120
Reflection losses R (%)	5.200
Polaron radius r_p (A°)	7.460
Inter-ionic distance r_i (A°)	18.800
Field strength F ($\times10^{14}$ cm^{-2})	5.400

3. Theoretical methods

3.1. Oscillator strengths: Judd–Ofelt theory

The Calculated oscillator strength of an $f-f$ transition can be evaluated by using the Judd – Ofelt theory [18,19]. According to this theory, the calculated oscillator strength of an induced electric-dipole transition from the ground state ΨJ, to an excited state $\Psi' J'$, is given by

$$f_{cal}=\frac{8\pi^2 mc\nu}{3h(2J+1)}\frac{(n^2+2)^2}{9n}\sum_{\lambda=2,4,6}\Omega_\lambda(\Psi J||U^\lambda||\Psi' J')^2 \quad (1)$$

where 'n' is refractive index of the medium and ν is the energy of the transition in cm^{-1}.

$(n^2+2)^2/9n$ is the Lorentz local field correction and accounts for dipole–dipole transition. J is the total angular momentum of the ground state, $\Omega_\lambda(\lambda=2,4$ and $6)$ are J–O intensity parameters and $||U^\lambda||^2$ are the doubly reduced matrix elements of the unit tensor operator [20] evaluated in the intermediate coupling scheme for a transition $\Psi J\rightarrow\Psi' J'$. The experimental oscillator strength of an absorption transition (f_{exp}) is directly proportional to the area under the absorption curve and is expressed as [13,21]

$$f_{exp}=\frac{2.303mc^2}{N\pi e^2}\int\varepsilon(\nu)d\nu=4.318\times10^{-9}\int\varepsilon(\nu)d\nu \quad (2)$$

where m and e are mass and charge of an electron, c is the velocity of light, N is the Avogadro's number, $\varepsilon(\nu)$ is the molar absorption coefficient of absorption band corresponding to the energy ν (cm^{-1}) and $d\nu$ is the half bandwidth. From the Beer–Lambert law, the molar absorption coefficient is given by

$$\varepsilon(\nu)=\frac{1}{Cl}\log\left(\frac{I_0}{I}\right) \quad (3)$$

where C is the rare-earth ion concentration (in mol/l), l is the thickness of the glass sample and $\log(I_0/I)$ is the optical density.

A least-squares fit method is then used for Eq. (1) to determine Ω_λ parameters, which gives the best fit between experimental and calculated oscillator strengths. The calculated oscillator strengths (f_{cal}) are then obtained using Eq. (1) and Ω_λ.

A measure of the accuracy of the fit between the experimental and calculated oscillator strengths is given by the root mean square (rms) deviation

$$\delta_{rms}=\left[\frac{\sum(f_{exp}-f_{cal})^2}{N}\right]^{1/2} \quad (4)$$

where N is the number of levels included in the fit. The small rms deviation indicates a good fit between experimental and calculated oscillator strengths.

3.2. Radiative properties

The radiative properties of excited states of Ln^{3+} ions are predicted by using the $J-O$ parameters along with refractive index (n). The radiative transition probability (A_R) for a transition $\Psi J \rightarrow \Psi' J'$ can be calculated from the following [22]

$$A_R(\Psi J, \Psi' J') = \frac{64\pi^4 \nu^3}{3h(2J+1)} \left[\frac{n(n^2+2)^2}{9} S_{ed} + n^3 S_{md}\right] \quad (5)$$

where S_{ed} and S_{md} are the electric and magnetic-dipole line strengths, respectively, calculated from the following [23,24]

$$S_{ed} = e^2 \sum_{\lambda = 2,4,6} \Omega_\lambda (\Psi J||U^\lambda||\Psi' J')^2 \quad (6)$$

$$S_{md} = \frac{e^2 h^2}{16\pi^2 m^2 c^2} (\Psi J||L+2S||\Psi' J')^2 \quad (7)$$

where $||U^\lambda||^2$ are the doubly reduced matrix elements of the unit tensor operator of rank $\lambda=2$, 4, and 6 calculated from the intermediate coupling scheme [25] and the Ω_λ are the host dependent J–O parameters. In our J–O analysis, we have utilized the reduced matrix elements and the S_{md} values reported by Jayasankar and Rukmini [20], since these matrix elements and S_{md} depend only on the RE ion but not on the host material. The S_{md} values also can be calculated using the formulae given elsewhere [23].

The radiative lifetime (τ_R) of an excited state is given by

$$\tau_R(\Psi J) = \frac{1}{\sum_{\Psi' J'} A_R(\Psi J, \Psi' J')} \quad (8)$$

The branching ratio (β_R) corresponding to the emission from an excited $\Psi' J'$ level to its lower level ΨJ is given by

$$\beta_R(\Psi J, \Psi' J') = \frac{A_R(\Psi J, \Psi' J')}{\sum_{\Psi' J'} A_R(\Psi J, \Psi' J')} \quad (9)$$

The branching ratios can be used to predict the relative intensities of all emission lines originating from a given excited state. The experimental branching ratios can be found from the relative areas of the emission bands.

The peak stimulated emission cross-section, $\sigma(\lambda p)(\Psi J, \Psi' J')$, between the emission levels ΨJ and $\Psi' J'$ having a probability of $A_R(\Psi J, \Psi'' J')$ can be expressed as

$$\sigma(\lambda p)(\Psi J, \Psi' J') = \frac{\lambda_p^4}{8\pi c n^2 \Delta\lambda_{eff}} A_R(\Psi J, \Psi' J') \quad (10)$$

where λp is the transition peak wavelength and $\Delta\lambda_{eff}$ is its effective line width found by dividing the area of the emission band by its average height.

3.3. Decay analysis

The measured lifetime (τ_m) of $^4G_{5/2}$ fluorescent level has been determined by taking first e-folding times of the decay curves. The measured lifetime (τ_m) can be expressed as [26]

$$\frac{1}{\tau_m} = \frac{1}{\tau_R} + W_{MP} + W_{ET} \quad (11)$$

where τ_m and τ_R are measured and radiative lifetimes obtained from the J–O theory, respectively. W_{MP} is the multi-phonon relaxation rate and W_{ET} is rate of energy transfer through cross-relaxation. But in case of Sm^{3+}, multi-phonon relaxation rate (W_{MP}) is negligible as there is a large energy gap of $\sim$7250 cm^{-1} between the fluorescent level $^4G_{5/2}$ and next lower level $^6G_{11/2}$. Hence, quenching of lifetimes with concentration may be mainly due to energy transfer through cross-relaxation (W_{ET}). Therefore,

$$W_{ET} = \frac{1}{\tau_m} - \frac{1}{\tau_R} \quad (12)$$

The quantum efficiency of the excited $^4G_{5/2}$ state η is given by

$$\eta = \frac{\tau_m}{\tau_R} \quad (13)$$

4. Results and discussion

4.1. XRD and FTIR spectral studies

In order to check the non-crystalline nature of the glass samples, the XRD measurement was performed for all samples and was similar to the 1.0 mol% Sm^{3+}-doped LCZSFB glass shown in Fig. 1. The results did not reveal any sharp peaks, therefore, the overall feature of the XRD pattern confirms the amorphous nature of the present glass.

The transmission spectrum of 1.0 mol% Sm^{3+}-doped LCZSFB glass in the IR region 450–4000 cm^{-1} is shown in Fig. 2. The peak at 497 cm^{-1} could be due to loose BO_4 units [27]. The bands at 708 and 975 cm^{-1} could be due to the bending and stretching vibrations of BO_4, while the peak around 1296 cm^{-1} is due to B–O stretching vibrations of BO_3 units [28]. The peak around 1636 cm^{-1} may be due to asymmetric stretching relaxation of the B–O bond of trigonal BO_3 units [29]. Similarly, the well known peaks in the region 2700–3400 cm^{-1} are due to OH bond vibrations [30].

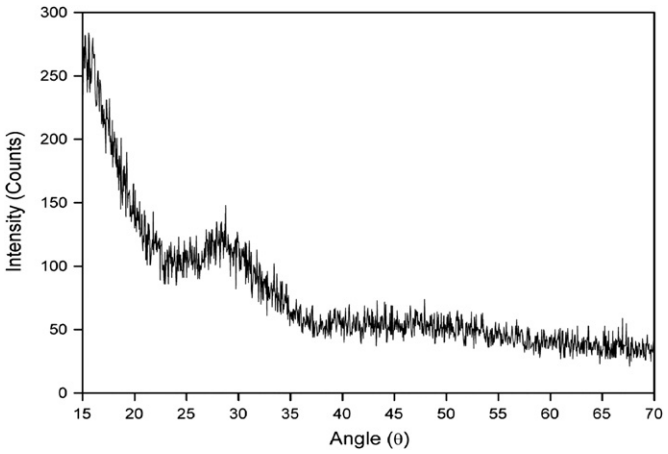

Fig. 1. XRD pattern of 1.0 mol% Sm^{3+}-doped LCZSFB glasses.

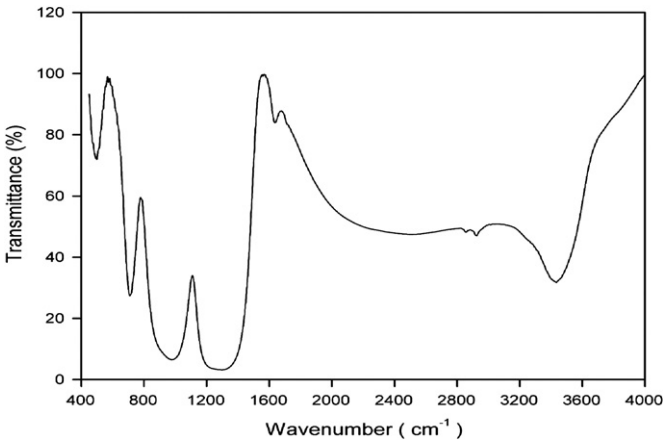

Fig. 2. FTIR spectrum of 1.0 mol% Sm^{3+}-doped LCZSFB glasses.

4.2. Optical absorption spectra

The optical absorption spectra of 1.0 mol% Sm^{3+}-doped LCZSFB glass measured at room temperature in visible and near infrared regions are shown in Figs. 3 and 4, respectively. Twelve discrete absorption bands observed from the absorption spectra are due to transition from $^6H_{5/2}$ ground level to the various excited $^{2S+1}L_J$ levels and are assigned to $^6H_{5/2}\rightarrow{}^6F_{1/2}$, $^6H_{15/2}$, $^6F_{3/2}$, $^6F_{5/2}$, $^6F_{7/2}$, $^6F_{9/2}$, $^6F_{11/2}$, $^4G_{5/2}$, $^4F_{3/2}$, $^4G_{7/2}$, $^4M_{15/2}$ and $^4I_{11/2}$ transitions at 6293, 6540, 6757, 7252, 8130, 9268, 10,582, 17,762, 18,939, 20,000, 21,052 and 21,645 cm^{-1}, respectively. The assignment of absorption transitions has been done based on the earlier literature [31]

The majority of the transitions in the spectra originate from induced electric dipole interactions with selection rule $\Delta J\leq 6$. Certain transitions also contain magnetic dipole contribution with selection rule $\Delta J=0, \pm 1$, for example the $^6H_{5/2}\rightarrow{}^4G_{5/2}$ transition at 563 nm [32]. In the visible region, all the transitions are spin forbidden and hence the absorption bands are weak in intensity. The presence of PbO content may also decrease the intensity of the absorption peaks [1]. As the 4f electrons are very effectively shielded by the filled 5s and 5p shells, the distinct sharp and intense bands are found in the infrared region at energies lower than 11,000 cm^{-1}. These spin-allowed transitions ($\Delta S=0$) are assigned to $^6H_{5/2}\rightarrow{}^6H_J$ manifolds with $J=\frac{1}{2}, \frac{3}{2}, \frac{5}{2}, \frac{7}{2}$ and $\frac{11}{2}$, respectively [33].

The transition $^6H_{5/2}\rightarrow{}^6F_{1/2}$ is the hypersensitive transition for the Sm^{3+} ion, which obeys the selection rules $|\Delta S|=0$, $|\Delta L|\geq 0$ and $|\Delta J|\geq 0$. The first excited state $^6H_{7/2}$ is nearly 1100 cm^{-1} above the ground state, but no transitions starting from this level could be detected. In our present work, only 7 absorption bands in near infrared region are chosen to determine the *J–O* parameters in 1.0 mol% Sm^{3+}-doped LCZSFB glasses.

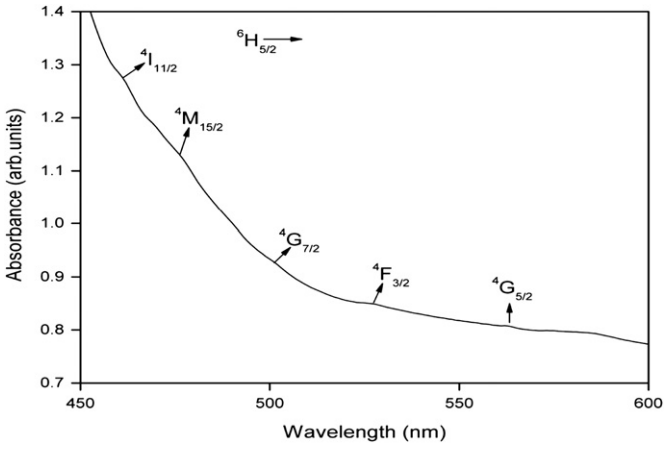

Fig. 3. VIS absorption spectra of 1.0 mol% Sm^{3+}-doped LCZSFB glasses.

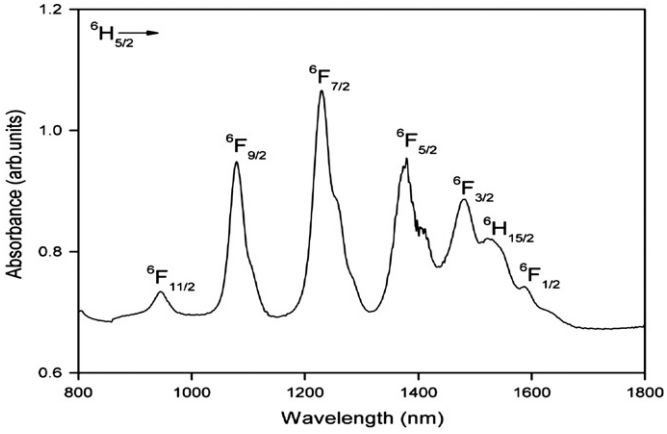

Fig. 4. NIR absorption spectra of 1.0 mol% Sm^{3+}-doped LCZSFB glasses.

4.3. Optical band gap

The optical band gap is an important parameter for describing solid-state materials. The optical band gap of glasses has been computed based on their UV absorption spectra, for understanding their optically induced transitions. The principle behind this technique is that a photon with energy greater than the band gap energy will be absorbed. The rapid rise in the absorption coefficient is referred to as the fundamental absorption edge (UV 'cut-off'). Normally, the optical absorption edge for disordered materials is interpreted in terms of indirect transitions across an optical band gap. The optical band gap is calculated from the absorption spectrum using the Tauc Eq. [34], $\alpha(\nu)=A[(h\nu-E_g)^2/h\nu]$ where $\alpha(\nu)$ is the absorption coefficient, A is a constant and E_g is the optical band gap determined by extrapolating from the linear region of plots of $(\alpha h\nu)^{1/2}$ against $h\nu$. The value of the optical band gap (E_g) is found to be 2.64 eV for 1.0 mol% Sm^{3+}-doped LCZSFB glass, which was determined by plotting the graph between $(\alpha h\nu)^{1/2}$ and $h\nu$ from the absorption spectrum as shown in Fig. 5.

4.4. Oscillator strengths and J–O intensity parameters

The intensity of an absorption band is expressed in terms of its oscillator strength [35]. From the absorption spectra the experimental oscillator strengths (f_{exp}) are determined by using Eq. (2). Calculated oscillator strengths (f_{cal}) and *J–O* intensity parameters are determined by using the least squares fit method to Eq. (1). The experimental and calculated oscillator strengths of observed absorption bands along with δ_{rms} deviation are tabulated in Table 2. The small δ_{rms} deviation of 0.76×10^{-6} between the experimental and calculated oscillator strengths of the absorption bands indicates a good fit. The derived *J–O* parameters are $\Omega_2=3.29\times10^{-20}$ cm^2, $\Omega_4=9.16\times10^{-20}$ cm^2 and $\Omega_6=5.28\times10^{-20}$ cm^2. The tendency of the *J–O* parameters in the present glass is found to be in the order $\Omega_4>\Omega_6>\Omega_2$. These *J–O* parameters are host dependent and are important for the investigation of glass structure, transition rates of rare-earth ion energy levels and bonding in the vicinity of RE ions. Table 3 presents the comparison of *J–O* intensity parameters, their trend and spectroscopic quality factors of Sm^{3+} ions in LCZSFB glass with different hosts.

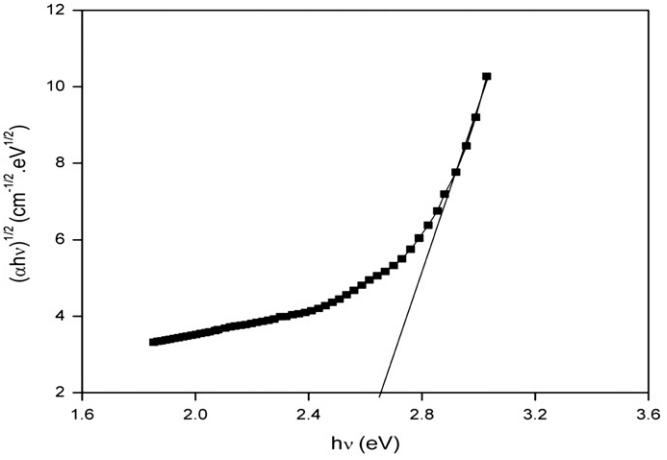

Fig. 5. Plot of $(\alpha h\nu)^{1/2}$ versus $h\nu$ for 1.0 mol% Sm^{3+}-doped LCZSFB glasses.

Table 2
Experimental and calculated oscillator strengths ($\times 10^{-6}$) for 1.0 mol% Sm^{3+}-doped LCZSFB glass.

Transition	Energy (cm^{-1})	f_{exp}	f_{cal}
$^6H_{5/2} \rightarrow {}^6F_{1/2}$	6293	0.57	1.03
$^6H_{15/2}$	6540	1.74	0.04
$^6F_{3/2}$	6757	3.74	3.01
$^6F_{5/2}$	7252	4.77	5.08
$^6F_{7/2}$	8130	7.32	7.53
$^6F_{9/2}$	9268	4.97	4.78
$^6F_{11/2}$	10,582	1.26	0.76
		$\delta_{rms} = \pm 0.76 \times 10^{-6}$	

Table 3
Comparison of *J–O* intensity parameters ($\times 10^{-20}$ cm^2), their trends and spectroscopic quality factors ($X = \Omega_4/\Omega_6$) for Sm^{3+} ion in different glass hosts.

Glass system	Ω_2	Ω_4	Ω_6	Trend	$X = \Omega_4/\Omega_6$
LCZSFB [present glass]	3.29	9.16	5.28	$\Omega_4 > \Omega_6 > \Omega_2$	1.75
L5FBS [26]	2.34	7.54	5.40	$\Omega_4 > \Omega_6 > \Omega_2$	1.40
ZBLAN [33]	2.15	3.05	1.56	$\Omega_4 > \Omega_6 < \Omega_2$	1.96
BPS30 [36]	2.96	5.73	3.25	$\Omega_4 > \Omega_6 > \Omega_2$	1.76
Fluorozirconate [39]	2.37	4.24	2.99	$\Omega_4 > \Omega_6 > \Omega_2$	1.41
NPCS [40]	2.18	3.80	2.15	$\Omega_4 > \Omega_6 < \Omega_2$	1.76
PKFBAS [41]	1.50	3.75	1.89	$\Omega_4 > \Omega_6 > \Omega_2$	1.98
PbO–PbF_2–B_2O_3 [42]	1.28	2.78	1.97	$\Omega_4 > \Omega_6 > \Omega_2$	1.41
PbO–PbF_2 [43]	1.16	2.60	1.40	$\Omega_4 > \Omega_6 > \Omega_2$	1.86

In general, the intensity parameter Ω_2 is related to the covalency, structural change and symmetry of ligand field around the Sm^{3+} site [36]. On the other hand, Ω_4 and Ω_6 values depend on the bulk properties such as viscosity and dielectric of the media and are also affected by the vibronic transitions of the RE ions bound to the ligand atoms [37]. Among the three Ω_λ parameters the value of Ω_2 is relatively large for oxide glasses, smaller for fluoride glasses while intermediate values are noticed for oxyfluoride glasses. This implies that Ln–O covalency decreases when pure oxide glasses are modified with fluorine content [38]. Thus, the higher magnitude of Ω_2 in the present work indicates the increase of covalent bonding and suggests that the Sm^{3+} ion possess higher site symmetry in LCZSFB glass host. Jacob and Weber [38] reported that the magnitude of spectroscopic quality factor $X = \Omega_4/\Omega_6$ is used to characterize the stimulated emission in any host glass matrix. The reasonably high value of spectroscopic quality factor $X = 1.75$ predicts efficient stimulated emission in the present host, and is comparable to other Sm^{3+}-doped glass systems as presented in Table 3. Once the values of Ω_λ are obtained, the other radiative parameters such as electric dipole line strength (S_{ed}), magnetic dipole line strength (S_{md}), spontaneous transition probabilities (A_R), total transition probability (A_T), radiative lifetime(τ_R) and branching ratios (β_R) corresponding to different emission channels from $^4G_{5/2}$ level have also been calculated using Eqs. (5)–(9) and are presented in Table 4.

4.5. Luminescence analysis and radiative properties

Fig. 7 shows the photoluminescence spectra of LCZSFB glasses doped with different concentrations of Sm^{3+} (0.1, 0.25, 0.5, 1.0 and 2.0 mol%) at room temperature in the spectral region 500–750 nm with an excited wavelength of 402 nm corresponding to $^6H_{5/2} \rightarrow {}^4F_{7/2}$ transition. The Fig. 6 represents the excitation spectrum of 1.0 mol% of Sm^{3+}-doped LCZSFB glass that consists of a sharp band at 402 nm wavelength. The fluorescence spectra exhibits four emission bands at 565, 602, 648 and 710 nm which

Table 4
Radiative properties such as peak emission wavelength (λ_P) electric (S_{ed}, $\times 10^{-22}$ cm^2) and magnetic (S_{md}, $\times 10^{-22}$ cm^2) dipole line strengths, radiative transition probabilities (A_R, s^{-1}), total radiative transition probability (A_T, s^{-1}), radiative lifetimes (τ_R, ms) and branching ratios (β_R) for 1.0 mol% Sm^{3+}-doped LCZSFB glass.

Transition	λ_P (nm)	S_{ed}	S_{md}	A_R	β_R
$^4G_{5/2} \rightarrow {}^6F_{11/2}$	–	0.35	0	0.64	0.001
$^6F_{9/2}$	–	0.97	0	2.93	0.005
$^6F_{7/2}$	–	1.66	0.27	8.60	0.014
$^6F_{5/2}$	–	3.92	0.66	26.20	0.043
$^6F_{3/2}$	–	0.45	0.85	9.00	0.015
$^6H_{15/2}$	–	0.11	0	0.70	0.001
$^6F_{1/2}$	–	0.33	0	2.26	0.004
$^6H_{13/2}$	–	1.13	0	10.70	0.018
$^6H_{11/2}$	710	5.96	0	72.59	0.120
$^6H_{9/2}$	648	10.87	0	173.50	0.288
$^6H_{7/2}$	602	12.61	0.58	264.88	0.440
$^6H_{5/2}$	565	0.65	0.57	31.02	0.051
		$A_T = 603$	$\tau_R = 1.66$		

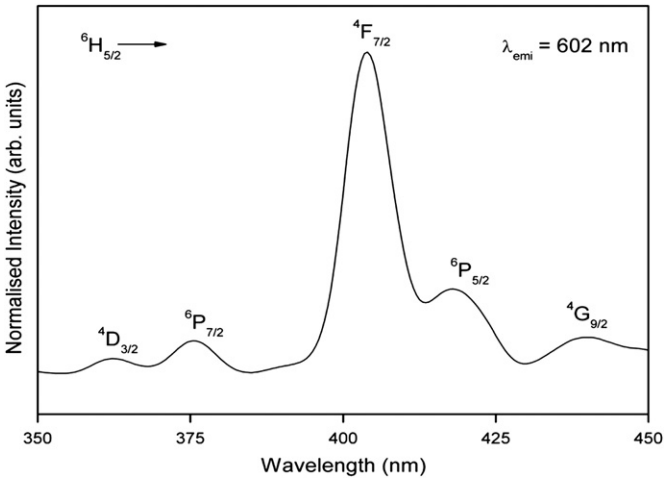

Fig. 6. Excitation spectrum of 1.0 mol% Sm^{3+}-doped LCZSFB glasses.

Table 5
Peak emission wavelength (λ_P), effective line width($\Delta\lambda_{eff}$, nm), radiative transition probabilities (A_R, s^{-1}), stimulated emission cross-section ($\sigma(\lambda_P)$, $\times 10^{-22}$ cm^2) experimental (β_m) and calculated branching ratios (β_R)) for 1.0 mol% Sm^{3+}-doped LCZSFB glass.

Transition	λ_P(nm)	$\Delta\lambda_{eff}$	$\sigma(\lambda_P)$	A_R	β_R	β_m
$^4G_{5/2} \rightarrow {}^6H_{11/2}$	710	20.60	4.70	72.59	0.12	0.06
$^6H_{9/2}$	648	19.32	8.30	173.50	0.29	0.19
$^6H_{7/2}$	602	14.49	12.60	264.88	0.44	0.59
$^6H_{5/2}$	565	13.85	1.20	31.02	0.05	0.21

are assigned to $^4G_{5/2} \rightarrow {}^6H_{5/2}$, $^6H_{7/2}$, $^6H_{9/2}$ and $^6H_{11/2}$ transitions, respectively. Among these four transitions $^4G_{5/2} \rightarrow {}^6H_{7/2}$ (602 nm) exhibit intense orange luminescence and $^4G_{5/2} \rightarrow {}^6H_{11/2}$ (710 nm) is a feeble one. The other two transitions, $^4G_{5/2} \rightarrow {}^6H_{5/2}$ (565 nm) and $^6H_{9/2}$ (648 nm) show moderate luminescence in the visible region.

The radiative transition rates (A_R), effective emission bandwidths ($\Delta\lambda_{eff}$), stimulated emission cross sections ($\sigma(\lambda p)$), branching ratios (β_R) and measured branching ratios (β_m) have been determined for the $^4G_{5/2}$ level of 1.0 mol% Sm^{3+}-doped, and are presented in Table 5. From the values of radiative transition probabilities of Table 5, it is noted that $^4G_{5/2} \rightarrow {}^6H_{7/2}$ transition

has highest radiative transition rate compared to other transitions. Hence, this transition is very useful for laser emission. The predicted branching ratios are found to be high for those transitions having maximum A_R values. The levels having the relatively large values of A_R, β_R and energy gap to the next lower level may exhibit laser action. With the relative areas under the emission peaks, the measured branching ratios (β_m) have been estimated for the $^4G_{5/2} \rightarrow {}^6H_J$ ($J' = \frac{5}{2}, \frac{7}{2}, \frac{9}{2}$ and $\frac{11}{2}$) transitions and the results are presented in Table 5. There is a reasonable agreement between measured and calculated branching ratios. The branching ratios of three emission transitions $^4G_{5/2} \rightarrow {}^6H_{5/2}$, $^6H_{7/2}$ and $^6H_{9/2}$ were found to be nearly 21%, 59% and 19%, respectively. The contribution of these transitions to the total branching ratio is nearly 99%, thereby suggesting that these transitions have the most potential for visible laser action for 1.0 mol% Sm^{3+} ions in LCZSFB glass.

From the fluorescence spectra, it is noted that the fluorescence intensity increases with increase in concentration from 0.1 to 1.0 mol% and beyond 1.0 mol% concentration quenching is observed. It is also found that the emission peak positions are unchanged for all concentrations (Fig. 7). When any of the energy levels above $^4G_{5/2}$ is excited, there is a quick non-radiative relaxation to this $^4G_{5/2}$ level due to the small energy gaps between them, and finally populate the $^4G_{5/2}$ level, from which the fluorescence of $^4G_{5/2} \rightarrow {}^6H_{5/2}$, $^6H_{7/2}$, $^6H_{9/2}$ and $^6H_{11/2}$ levels takes place. The corresponding partial energy level diagram of Sm^{3+} doped LCZSFB glasses and their emission transitions has been depicted in Fig. 9. The $^4G_{5/2}$ level possess purely radiative relaxation as this level has sufficient energy gap of $\approx 7250\ cm^{-1}$ with respect to next lower level $^6F_{11/2}$. The radiative relaxation of an excited state to all its lower levels depends upon A_R values. The values of A_R depend upon J–O parameters and energy gap between initial and terminal levels. The stimulated emission cross-section $\sigma(\lambda p)$ is an important parameter and its value signifies that the rate of energy extraction from the lasing material. The large stimulated emission cross-sections are the attractive features for low-threshold, high gain laser applications, which are utilized to obtain CW laser action [44]. The values of $\sigma(\lambda p)$ for the $^4G_{5/2}$ emission transitions are in the order of $^4G_{5/2} \rightarrow {}^6H_{7/2} > {}^6H_{9/2} > {}^6H_{11/2} > {}^6H_{5/2}$. The stimulated emission cross-section $\sigma(\lambda p)$ of $12.6 \times 10^{-22}\ cm^2$ estimated for the $^4G_{5/2} \rightarrow {}^6H_{7/2}$ intense emission band of 1.0 mol% of Sm^{3+}-doped LCZSFB glass and is compared with the other reported values [1,25,42,45]. Thus, reasonably high values of $\sigma(\lambda p)$ suggest that the present glasses can be used for high gain laser applications.

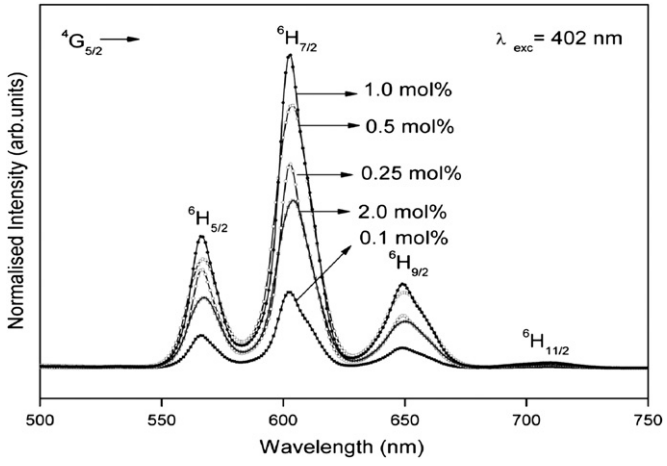

Fig. 7. Fluorescence spectra for different concentrations of Sm^{3+}-doped LCZSFB glasses.

4.6. Fluorescence lifetimes

The lifetimes of the $^4G_{5/2}$ level has been measured at room temperature for the glass samples containing 0.1, 0.25, 0.5, 1.0 and 2.0 mol% of Sm^{3+} ions. The measured lifetime (τ_m) of excited $^4G_{5/2}$ level has been determined by taking first e-folding times of the decay curves [46]. It is observed that the lifetime is strongly depends upon the Sm^{3+} ion concentration. In lower concentration sample (0.1 and 0.25 mol%), the decay curve shown in Fig. 8 is well fitted to a single exponential which indicates the absence of energy transfer among the Sm^{3+} ions. However, for the samples with higher concentrations (0.5, 1.0 and 2.0 mol%), the fluorescence decay becomes non-exponential due to non-radiative energy transfer of the excited ions as shown in Fig. 8.

In the present glasses, the measured lifetime of excited states τ_m significantly decreases with increase of Sm^{3+} ion concentration due to energy transfer [47] as presented in Table 6. The decrease of lifetime and the departure from the exponential law are characteristic of the existence of a concentration quenching mechanism in the lifetime of $^4G_{5/2}$ level at higher concentrations. The τ_m values are significantly smaller than the predicted values 1.66 ms obtained using the J–O theory. These drastic changes may be due to the energy transfer through cross-relaxation [26] but not due to the multi-phonon relaxation as it is negligible in case of Sm^{3+}, since the energy gap is very large ($7250\ cm^{-1}$) between $^4G_{5/2}$ and next lower level $^6F_{11/2}$. The magnitude of energy transfer rate can be calculated by using the Eq. (12) and is of $462\ s^{-1}$ for the $^4G_{5/2}$ level of 1.0 mol% Sm^{3+}-doped LCZSFB glass which indicates high non-exponential nature than those of other Sm^{3+}-doped glass matrices [13,26,41]. One of the possible mechanisms for the fluorescence quenching is the cross-relaxation of ($^4G_{5/2}$, $^6H_{5/2}$)→ ($^6F_{5/2}$, $^6F_{11/2}$) transitions as the energy differences between these transitions are negligible. This cross-relaxation is due to energy transfer from the excited $^4G_{5/2}$ energy state to the nearby Sm^{3+}

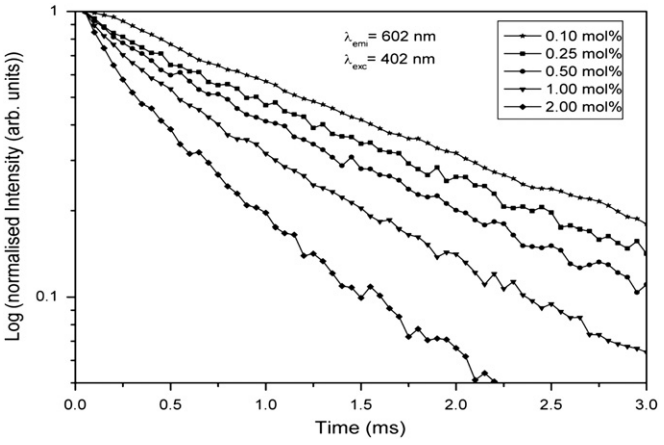

Fig. 8. The decay profiles of $^6H_{7/2}$ level for different concentrations of Sm^{3+} ions in LCZSFB glasses.

Table 6
Variation of lifetime (τ_m, ms), quantum efficiency (η, %) and energy transfer rate (W_{ET}, s^{-1}) with respect to concentration (mol%) of Sm^{3+} ions in LCZSFB glasses.

Concentration	Lifetime(ms)	η	W_{NR}
0.10	1.61	97	19
0.25	1.48	89	73
0.50	1.24	75	204
1.00	0.94	57	462
2.00	0.59	36	1093

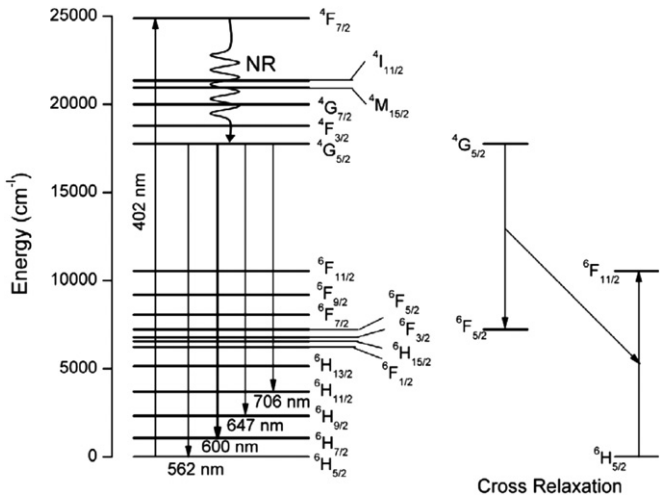

Fig. 9. Energy level diagram showing cross-relaxation channel for Sm^{3+}-doped LCZSFB glasses.

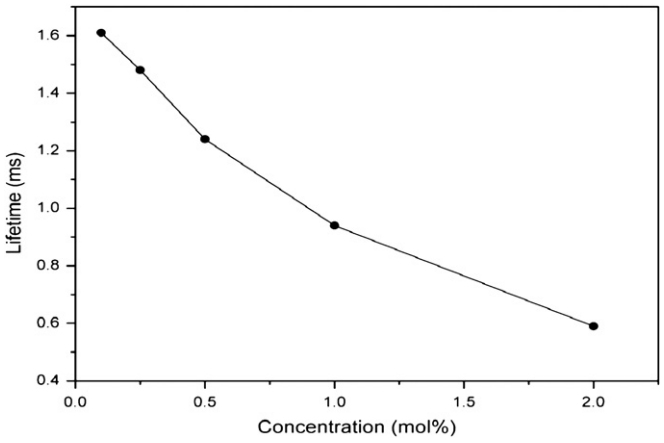

Fig. 10. Variation of measured lifetimes for $^4G_{5/2}$ level of Sm^{3+} ions with concentration in LCZSFB glasses.

ions in $^6H_{5/2}$ ground state. This transfer of cross-relaxation occurs via $^4G_{5/2} \rightarrow {}^6F_{5/2}$ transition on one ion and $^6H_{5/2} \rightarrow {}^6F_{11/2}$ transition on the other. After that, both ions quickly decay non-radiatively to the ground state [47]. The energy resonance of these transitions can be clearly seen in Fig. 9. The variation of lifetime with concentration is shown in Fig. 10.

The quantum efficiency of the fluorescent level is defined as the ratio of the number of photons emitted to the number of photons absorbed and was calculated by using Eq. (13). In the present case, the quantum efficiency is estimated to be 57% for 1.0 mol% Sm^{3+}-doped LCZSFB glass and for remaining concentrations, the values are noted in Table 6.

5. Conclusions

The absorption and fluorescence studies of Sm^{3+} ions doped in LCZSFB glasses have been studied. From the analysis of optical absorption and photoluminescence studies, the *J–O* intensity parameters, radiative transition rates, branching ratios, radiative lifetimes and stimulated emission cross-sections are calculated and are found to be comparable with other reported values. From the decay curves, it is concluded that the lifetime of $^4G_{5/2}$ level has been found to depend strongly on the concentration of Sm^{3+} ions and glass composition. In present case, lifetime of the $^4G_{5/2}$ level has been found to decrease with increasing concentrations of Sm^{3+} ions. At lower concentrations the decay curves are perfectly single-exponential and become non-exponential for higher concentrations. The decrease of lifetime at higher concentrations is due to the energy transfer through the cross-relaxation. Usually, a good material for a laser emission should have large stimulated emission cross-sections, high branching ratios and quantum efficiencies. Based on the physical and optical properties such as strong visible emissions, large stimulated emission cross-sections and high branching ratios, it is concluded that 1.0 mol% Sm^{3+} ions doped LCZSFB glass may be used as luminescent novel optical materials for the development of lasers and photonic devices operating in the visible region.

Acknowledgement

The authors acknowledge the Sophisticated Analytical Instrument Facility (SAIF), IIT, Chennai for extending instrumental facilities.

References

[1] P. Srivastava, S.B. Rai, D.K. Rai, Spectrochim. Acta. Part A. 60 (2004) 637.
[2] E.A. dos Santos, L.C. Courrol, L.R.P. Kassab, L. Gomes, N.U. Wetter, J.N.D. Vieira, J.L. Ribeiro, Y. Messaddeq, J. Lumin. 124 (2007) 200.
[3] S. Murugesan, B. Bergman, Electrochim. Acta. 52 (2007) 8064.
[4] B.K. Keller, M.D. Degrandpre, C.P. Palmer, Sensors and Actuators B 125 (2007) 360.
[5] A. Paul, R.W. Donglas, Phys. Chem. Glasses. 6 (1965) 212.
[6] J.L. Piguet, J.E. Shelly, J. Am. Ceram. Soc. 68 (1985) 450.
[7] K.S.V. Sudhakar, M. Srinivasa Reddy, L. Srinivasa Rao, N. Veeraiah, J. Lumin. 128 (2008) 1791.
[8] L. Srinivasa Rao, M. Srinivasa Reddy, M.V. Ramana Reddy, N. Veeraiah, Physica B. 403 (2008) 2542.
[9] M. Naftaly, A. Jha, J. Appl. Phys. 87 (2000) 2098.
[10] J.E. Marion, M.J. Weber, Eur. J. Solid State Inorg. Chem. 28 (1991) 271.
[11] M.R. Sahar, A.K. Jehbu, M.M. Karim, J. Non-Cryst. Solids. 213–214 (1997) 164.
[12] K.K. Mahato, D.K. Rai, S.B. Rai, Solid State Commun. 108 (1998) 671.
[13] V.D. Rodriguez, I.R. Martin, R. Alcala, R. Cases, J. Lumin. 54 (1992) 231.
[14] R. Reisfeld, A. Bornstein, L. Boehm, J. Solid. State Chem. 14 (1975) 14.
[15] A. Kumar, D.K. Rai, S.B. Rai, Spectrochim. Acta Part A. 59 (2003) 917.
[16] M. Dejneka, E. Snitzer, R.E. Riman, J. Lumin. 65 (1995) 227.
[17] R. Van Deun, K. Binnemans, C. Gorller-Walrand, J.L. Adam, J. Alloy. Compd. (1999) 59283 (1999) 59.
[18] B.R. Judd, Phys. Rev. 127 (1962) 750.
[19] G.S. Ofelt, J. Chem. Phys. 37 (1962) 511.
[20] C.K. Jayasankar, E. Rukmini, Opt. Mater. 8 (1997) 193.
[21] C. Gorller-Walrand, K. Binnemans, in: K.A. Gschneidner Jr., L. Eyring (Eds.), Handbook on the physics and chemistry of rare earths, 25, North-Holland, Amsterdam, 1998, pp. 101–264 (Chapter 167).
[22] W.T. Carnall, P.R. Fields, K. Rajnak, J. Chem. Phys. 49 (1968) 4412.
[23] W.T. Carnall, P.R. Fields, B.G. Wybourne, J. Chem. Phys. 42 (1965) 3797.
[24] M.J. Weber, D.C. Ziegler, C.A. Angell, J. Appl. Phys. 53 (1982) 4344.
[25] C.K. Jayasankar, P. Babu, J. Alloy. Compd. 307 (2000) 82.
[26] V. Venkatramu, P. Babu, C.K. Jayasankar, Th. Troster, W. Sievers, G. Wortmann, Opt. Mater. 29 (2007) 1429.
[27] N. Syam Prasad, K.B.R. Varma, Mater. Sci. Eng. B90 (2002) 246.
[28] S.G. Motke, S.P. Yawale, S.S. Yawale, Bull. Mater. Sci. 25 (2002) 75.
[29] G. Lakshminarayana, S. Buddhudu, Spectrochim. Acta Part A. 62 (2005) 364.
[30] J. Suresh Kumar, K. Pavani, A. Mohan Babu, Neeraj Kumar Giri, S.B. Rai, L. Rama Moorthy, J. Lumin. 130 (2010) 1916.
[31] B.C. Jamalaiah, J. Suresh Kumar, A. Mohan Babu, T. Suhasini, L. Rama Moorthy, J. Lumin. 129 (2009) 363.
[32] R. Van Deun, K. Binnemans, C. Gorller Walrand, J.L. Adam, SPIE 3622 (1999) 175.
[33] L.J.F. Broer, C.J. Gorter, J. Hoogschagen, Physica 11 (1945) 231.
[34] R. Jose, T. Suzuki, Y. Ohishi, J. Non-Cryst. Solids 352 (2006) 5564.
[35] M.B. Saisudha, J. Ramakrishna, Phys. Rev. B 53 (1996) 6186.
[36] S. Tanabe, T. Ohayagi, N. Soga, T. Hanada, Phys. Rev. B 46 (1992) 3305.
[37] W.F. Krupke, Phys. Rev. 145 (1966) 325.
[38] R.R. Jacobs, M.J. Weber, IEEE J. Quantum Electron. 12 (1976) 102.
[39] M. Canalejo, R. Cases, R. Alcala, Phys. Chem. Glasses 29 (1988) 187.
[40] K. Binnemans, R. Van Deun, C. Gorller-Walrand, J.L. Adam, J. Non-Cryst. Solids 238 (1998) 11–29.
[41] T. Suhasini, J. Suresh Kumar, T. Sasikala, Kiwan Jang, Ho Sueb Lee, M. Jayasimhadri, Jung Hyun Jeong, Soung Soo Yi, L. Rama Moorthy, Opt. Mater. 31 (2009) 1167–1172.

[42] A.G.S. Filho, P.T.C. Freire, I. Guedes, F.E.A. Melo, J.M. Filho, M.C.C. Custodio, R. Lebullenger, A.C. Hernandes, J. Mater. Sci. Lett. 19 (2000) 135.
[43] P. Nachimuthu, R. Jagannatham, V. Nirmal Kumar, D. Narayana Rao, J. Non-Cryst. Solids 217 (1997) 215.
[44] M.B. Saisudha, J. Ramakrishna, Opt. Mater. 18 (2002) 403–417.
[45] M. Jayasimhadri, L.R. Moorthy, S.A. Saleem, R.V.S.S.N. Ravi Kumar, Spectrochim. Acta. Part A. 64 (2006) 939.
[46] V.M. Orera, P.J. Alonso, R. Cases, R. Alcala, Phys. Chem. Glasses. 29 (1988) 59.
[47] S. Surendra Babu, C.K. Jayasankar, P. Babu, T. Troster, W. Sievers, G. Wortmann, Phys. Chem. Glasses 47 (2006) 548.